Boundary Value Problems
a SpringerOpen Journal

RESEARCH Open Access

Legendre spectral collocation method for distributed and Riesz fractional convection–diffusion and Schrödinger-type equation

M.A. Abdelkawy[1,2*], Mdi Begum Jeelani[1], Abeer S. Alnahdi[1], T.M. Taha[2] and E.M. Soluma[1,2]

*Correspondence:
maohamed@imamu.edu.sa;
melkawy@yahoo.com
[1]Department of Mathematics and Statistics, Faculty of Science, Imam Mohammad Ibn Saud Islamic University, Riyadh, Saudi Arabia
[2]Department of Mathematics, Faculty of Science, Beni-Suef University, Beni-Suef, Egypt

Abstract

The numerical analysis of the temporal distributed and spatial Riesz fractional problem (TDSRFP) is presented in this work. To address the two independent variables, the suggested technique employs a completely spectral Legendre collocation approach. For the current model, our technique is proven to be more accurate, efficient, and practical. The results confirmed that the spectral scheme is exponentially convergent.

Keywords: Spectral collocation method; Distributed fractional; Riesz fractional

1 Introduction

As it is more appropriate for modeling many real-world situations than the classical derivative [1–3], the notion of fractional derivatives [4–9] has become one of the most important topics in applied mathematics. The major reason is that it is widely utilized in fields like chemistry [10], biology [11], physics [12], engineering, and finance. In the mathematical literature, fractional derivatives are defined in a variety of ways, including the Riemann–Liouville and Caputo fractional senses.

The anomalous diffusion [13, 14] and relaxation processes have been thoroughly described using distributed fractional problems, which are an extension of single-term and multi-term problems. Chechkin et al. [15] were the first to list them, and they were thereafter widely used to characterize the phenomena of diffraction and relaxation, i.e., the heating and cooling of objects in a thermal or magnetic field. Mashayekhi and Razzaghi [16] solved temporal distributed fractional differential equations using the Riesz fractional derivative, which is one of the key definitions of the spatial fractional derivative in quantum mechanics [17]. To solve quantum mechanical problems, block-pulse functions and Bernoulli polynomials, as well as Fourier transformations, have been employed. Chen et al. [18] solved the one-dimensional temporal distributed fractional reaction-diffusion equation with unbounded domain, while the replicating kernel technique [19] was used to solve the temporal distributed fractional diffusion equation with variable coefficients. To solve

© The Author(s) 2022. This article is licensed under a Creative Commons Attribution 4.0 International License, which permits use, sharing, adaptation, distribution and reproduction in any medium or format, as long as you give appropriate credit to the original author(s) and the source, provide a link to the Creative Commons licence, and indicate if changes were made. The images or other third party material in this article are included in the article's Creative Commons licence, unless indicated otherwise in a credit line to the material. If material is not included in the article's Creative Commons licence and your intended use is not permitted by statutory regulation or exceeds the permitted use, you will need to obtain permission directly from the copyright holder. To view a copy of this licence, visit http://creativecommons.org/licenses/by/4.0/.

one- and multi-dimensional distributed-order diffusion equations, spectral Galerkin [20] and collocation [21–25] have been used. Liu et al. [26] used a finite volume technique, Fan and Liu [27] used a finite element method, and Jia and Wang [28] utilized a fast finite difference method for distributed fractional differential problems in space variables. Another case is the use of anomalous diffusion, the issue in which the Riesz derivative indicates nonlocality and is used to represent the dependency of diffusion concentration on route. Fractional differential equations with the Riesz derivative are required to describe this type of phenomena. Riesz derivatives are two-sided fractional operators that have both left and right derivatives. This capability is especially useful for fractional modeling on finite domains. There is limited literature on fractional differential equations with the Riesz derivative. Chen et al. [29] investigated the existence of Riesz-fractional differential equations in the Caputo sense. In [30], the time-space Riesz fractional advection-diffusion equations were solved using the finite difference method. Riesz–Caputo variational optimal problems have been discussed by Agrawal [31]. Noether's theorem for Riesz–Caputo fractional variational problems has been established by Frederico and Torres [32]. Almeida [33] investigated optimality criteria for Riesz–Caputo variational problems. Various numerical techniques [34–38] have been developed to handle Riesz Riemann–Liouville derivative fractional issues. Wang et al. [39] also used a second-order finite difference approach to solve the linear Riesz-distributed advection-dispersion issue. Fan et al. [27] mentioned the finite element technique for two-dimension linear Riesz-distributed diffusion problem on an irregular convex domain. To solve Riesz-distributed problems, finite volume techniques were utilized in [26, 40].

Spectral techniques [41–44] are effective tools for solving many sorts of differential [45, 46] and integral equations encountered in science and engineering [47–50]. Because explicit analytical solutions to space and/or time-fractional differential equations are in most circumstances impossible to acquire, creating efficient numerical methods is a high priority. There has been significant growth in fractional differential and integral equations due to their high-order accuracy. Compared to the effort put into analyzing finite difference schemes in the literature for solving the fractional-order differential equations, only a little work has been put into developing and analyzing global spectral schemes [51–53]. The primary goal of this work is to develop the Gauss–Lobatto Legendre collection technique (GLLCT) and the Gauss–Radu shifted Legendre collection technique (GRSLCT) for handling spatial and temporal variables.

The following is a description of the paper's structure. The numerical approach for solving the TDSRFP is presented in Sect. 2. Section 3 solves and analyzes three cases to demonstrate the method's efficiency and correctness. The major conclusions are outlined in Sect. 4.

2 Spectral collocation treatment

2.1 Distributed and Riesz fractional convection–diffusion equation

To tackle the TDSRFP of the form, GLLCT and GRLCT are suggested.

$$\int_0^1 \kappa(\mu)\,{}_0^c\mathcal{D}_t^{\mu}\mathcal{U}(x,t)\,d\mu + \varepsilon(-\Delta)^{\frac{\delta}{2}}\mathcal{U}(x,t) = \Lambda\big(x,t,\mathcal{U}(x,t)\big), \quad (x,t)\in\Lambda^{\bullet}\times\Lambda^{\diamond}, \tag{2.1}$$

where $\Lambda^{\bullet} \equiv [-1,1]$ and $\Lambda^{\diamond} \equiv [0, t_{\text{end}}]$. Related to

$$\begin{aligned} &\mathcal{U}(x,0) = \Theta_1(x), \quad x \in \Lambda^{\bullet}, \\ &\mathcal{U}(0,t) = \Theta_2(t), \qquad \mathcal{U}(x_{\text{end}},t) = \Theta_3(t), \quad t \in \Lambda^{\diamond}. \end{aligned} \tag{2.2}$$

To convert the TDSRFP into a nonlinear algebraic system, the GLLCT and GRSLCT are used. The truncated solution is written as

$$\mathcal{U}_{\mathcal{N},\mathcal{M}}(x,t) = \sum_{\substack{r_1=0,\ldots,\mathcal{N} \\ r_2=0,\ldots,\mathcal{M}}} \varsigma_{r_1,r_2} \mathcal{G}_{r_1}(x) \mathcal{G}^{t_{\text{end}}}_{r_2}(t), \tag{2.3}$$

where $\mathcal{G}_{r_1}(x)$ and $\mathcal{G}^{t_{\text{end}}}_{r_2}(t)$ are the Legendre and shifted Legendre polynomials, see [54, 55] for more details. $(-\Delta)^{\frac{\delta}{2}}\mathcal{U}(x,t)$ is calculated as follows:

$$\begin{aligned} (-\Delta)^{\frac{\delta}{2}}\mathcal{U}(x,t) &= -\frac{1}{2\cos(\frac{\pi\delta}{2})}\left({}^{c}_{-1}\mathcal{D}^{\delta}_{x}\mathcal{U}(x,t) + {}^{c}_{x}\mathcal{D}^{\delta}_{1}\mathcal{U}(x,t)\right) \\ &= -\frac{1}{2\cos(\frac{\pi\delta}{2})}\left(\sum_{\substack{r_1=0,\ldots,\mathcal{N} \\ r_2=0,\ldots,\mathcal{M}}} \varsigma_{r_1,r_2}\left({}^{c}_{-1}\mathcal{D}^{\delta}_{x}\mathcal{G}_{r_1}(x) + {}^{c}_{x}\mathcal{D}^{\delta}_{1}\mathcal{G}_{r_1}(x)\right)\mathcal{G}^{t_{\text{end}}}_{r_2}(t)\right) \\ &= \sum_{\substack{r_1=0,\ldots,\mathcal{N} \\ r_2=0,\ldots,\mathcal{M}}} \varsigma_{r_1,r_2} \mathcal{G}^{\Delta}_{r_1}(x) \mathcal{G}^{t_{\text{end}}}_{r_2}(t), \end{aligned} \tag{2.4}$$

where $\mathcal{G}^{\Delta}_{r_1}(x) = -\frac{1}{2\cos(\frac{\pi\delta}{2})}\left({}^{c}_{-1}\mathcal{D}^{\delta}_{x}\mathcal{G}_{r_1}(x) + {}^{c}_{x}\mathcal{D}^{\delta}_{1}\mathcal{G}_{r_1}(x)\right)$, see [56, 57] for Riesz fractional derivative definition.

The Caputo fractional derivative ${}^{c}_{0}\mathcal{D}^{\mu}_{t}\mathcal{U}(x,t)$ is computed as

$${}^{c}_{0}\mathcal{D}^{\mu}_{t}\mathcal{U}(x,t) = \sum_{\substack{r_1=0,\ldots,\mathcal{N} \\ r_2=0,\ldots,\mathcal{M}}} \varsigma_{r_1,r_2} \mathcal{G}_{r_1}(x) \mathcal{G}^{t_{\text{end}}}_{r_2,\mu}(t), \tag{2.5}$$

where $\mathcal{G}^{t_{\text{end}}}_{r_2,\mu}(t) = {}^{c}_{0}\mathcal{D}^{\mu}_{t}\mathcal{G}^{t_{\text{end}}}_{r_2}(t)$, see [58]. The integrated operator's treatment provides us with

$$\begin{aligned} \int_0^1 \kappa(\mu)\, {}^{c}_{0}\mathcal{D}^{\mu}_{t}\mathcal{U}(x,t)\, d\mu &= \int_0^1 \left(\kappa(\mu) \sum_{\substack{r_1=0,\ldots,\mathcal{N} \\ r_2=0,\ldots,\mathcal{M}}} \varsigma_{r_1,r_2} \mathcal{G}_{r_1}(x) \mathcal{G}^{t_{\text{end}}}_{r_2,\mu}(t)\right) d\mu \\ &= \sum_{\substack{r_1=0,\ldots,\mathcal{N} \\ r_2=0,\ldots,\mathcal{M}}} \varsigma_{r_1,r_2} \int_0^1 \kappa(\mu) \mathcal{G}_{r_1}(x) \mathcal{G}^{t_{\text{end}}}_{r_2,\mu}(t)\, d\mu \\ &= \sum_{\substack{r_1=0,\ldots,\mathcal{N} \\ r_2=0,\ldots,\mathcal{M} \\ r_3=0,\ldots,\mathcal{Q}}} \varsigma_{r_1,r_2} \mathcal{G}_{r_1}(x) \mathcal{F}^{t_{\text{end}}}_{r_2,r_3}(t), \end{aligned} \tag{2.6}$$

where $\mathcal{F}^{t_{\text{end}}}_{r_2,r_3}(t) = \varpi_{\mathcal{Q},r_3} \kappa(\mu_{\mathcal{Q},r_3}) \mathcal{G}^{t_{\text{end}}}_{r_2,\mu_{\mathcal{Q},r_3}}$ and $\mu_{\mathcal{Q},r_3}$, $r_3 = 0, 1, \ldots, \mathcal{Q}$ are the shifted Legendre Gauss–Lobatto collocation points in the interval $[0,1]$, see [54, 59, 60].

At selected nodes, the preceding derivatives are calculated as follows:

$$\left((-\Delta)^{\frac{\delta}{2}}\mathcal{U}(x,t)\right)^{x=x_{\mathcal{N},n},}_{t=t^{t_{\text{end}}}_{\mathcal{M},m}} = \sum_{\substack{r_1=0,\dots,\mathcal{N}\\ r_2=0,\dots,\mathcal{M}}} \varsigma_{r_1,r_2}\mathcal{G}^{\Delta}_{r_1}(x_{\mathcal{N},n})\mathcal{G}^{t_{\text{end}}}_{r_2}\left(t^{t_{\text{end}}}_{\mathcal{M},m}\right), \tag{2.7}$$

$$\left(\int_0^1 \kappa(\mu)\,{}^{c}_{0}\mathcal{D}^{\mu}_{t}\mathcal{U}(x,t)\,d\mu\right)^{x=x_{\mathcal{N},n},}_{t=t^{t_{\text{end}}}_{\mathcal{M},m}} = \sum_{\substack{r_1=0,\dots,\mathcal{N}\\ r_2=0,\dots,\mathcal{M}\\ r_3=0,\dots,\mathcal{Q}}} \varsigma_{r_1,r_2}\mathcal{G}_{r_1}(x_{\mathcal{N},n})\mathcal{F}^{t_{\text{end}}}_{r_2,r_3}\left(t=t^{t_{\text{end}}}_{\mathcal{M},m}\right), \tag{2.8}$$

where $n = 0, 1, \dots, \mathcal{N}$, $m = 0, 1, \dots, \mathcal{M}$ and $x_{\mathcal{N},n}$, $t^{t_{\text{end}}}_{\mathcal{M},m}$ are Gauss–Lobatto Legendre collocation and Gauss–Radau shifted Legendre collocation nodes, respectively.

Equation (2.1) is coerced to zero at the $(\mathcal{N}-1)\times(\mathcal{M})$ nodes in the approach.

$$\Omega\left(x_{\mathcal{N},n}, t^{t_{\text{end}}}_{\mathcal{M},m}\right) = \Lambda\left(x_{\mathcal{N},n}, t^{t_{\text{end}}}_{\mathcal{M},m}, \sum_{\substack{r_1=0,\dots,\mathcal{N}\\ r_2=0,\dots,\mathcal{M}}} \varsigma_{r_1,r_2}\mathcal{G}_{r_1}(x_{\mathcal{N},n})\mathcal{G}^{t_{\text{end}}}_{r_2}\left(t^{t_{\text{end}}}_{\mathcal{M},m}\right)\right), \tag{2.9}$$

where

$$\begin{aligned}\Omega\left(x_{\mathcal{N},n}, t^{t_{\text{end}}}_{\mathcal{M},m}\right) = {} & \sum_{\substack{r_1=0,\dots,\mathcal{N}\\ r_2=0,\dots,\mathcal{M}}} \varsigma_{r_1,r_2}\mathcal{G}^{\Delta}_{r_1}(x_{\mathcal{N},n})\mathcal{G}^{t_{\text{end}}}_{r_2}\left(t^{t_{\text{end}}}_{\mathcal{M},m}\right)\\ & + \varepsilon \sum_{\substack{r_1=0,\dots,\mathcal{N}\\ r_2=0,\dots,\mathcal{M}\\ r_3=0,\dots,\mathcal{Q}}} \varsigma_{r_1,r_2}\mathcal{G}_{r_1}(x_{\mathcal{N},n})\mathcal{F}^{t_{\text{end}}}_{r_2,r_3}\left(t^{t_{\text{end}}}_{\mathcal{M},m}\right).\end{aligned}$$

Otherwise, initial-boundary can be obtained by

$$\begin{aligned}&\sum_{\substack{l,r_1=0,\dots,\mathcal{N}\\ r_2=0,\dots,\mathcal{M}}} \varsigma_{r_1,r_2}\mathcal{G}_{r_1}(x)\mathcal{G}^{t_{\text{end}}}_{r_2}(0) = \Theta_1(x),\\ &\sum_{\substack{l,r_1=0,\dots,\mathcal{N}\\ r_2=0,\dots,\mathcal{M}}} \varsigma_{r_1,r_2}\mathcal{G}_{r_1}(-1)\mathcal{G}^{t_{\text{end}}}_{r_2}\left(t^{t_{\text{end}}}_{\mathcal{M},m}\right) = \Theta_2\left(t^{t_{\text{end}}}_{\mathcal{M},m}\right),\\ &\sum_{\substack{l,r_1=0,\dots,\mathcal{N}\\ r_2=0,\dots,\mathcal{M}}} \varsigma_{r_1,r_2}\mathcal{G}_{r_1}(1)\mathcal{G}^{t_{\text{end}}}_{r_2}\left(t^{t_{\text{end}}}_{\mathcal{M},m}\right) = \Theta_3(t).\end{aligned} \tag{2.10}$$

Therefore, adapting (2.1)–(2.10), we get

$$\Omega\left(x_{\mathcal{N},n}, t^{t_{\text{end}}}_{\mathcal{M},m}\right) = \Lambda\left(x_{\mathcal{N},n}, t^{t_{\text{end}}}_{\mathcal{M},m}, \sum_{\substack{r_1=0,\dots,\mathcal{N}\\ r_2=0,\dots,\mathcal{M}}} \varsigma_{r_1,r_2}\mathcal{G}_{r_1}(x_{\mathcal{N},n})\mathcal{G}^{t_{\text{end}}}_{r_2}\left(t^{t_{\text{end}}}_{\mathcal{M},m}\right)\right), \tag{2.11}$$

with $n = 1, \dots, \mathcal{N} - 1$, $m = 1, \dots, \mathcal{M}$, additionally

$$\begin{aligned}
&\sum_{\substack{l,r_1=0,\dots,\mathcal{N}\\ r_2=0,\dots,\mathcal{M}}} \varsigma_{r_1,r_2}\mathcal{G}_{r_1}(x_{\mathcal{N},n})\mathcal{G}_{r_2}^{t_{\text{end}}}(0) = \Theta_1(x_{\mathcal{N},n}), \quad k = 1, \dots, \mathcal{N} - 1,\\
&\sum_{\substack{l,r_1=0,\dots,\mathcal{N}\\ r_2=0,\dots,\mathcal{M}}} \varsigma_{r_1,r_2}\mathcal{G}_{r_1}(-1)\mathcal{G}_{r_2}^{t_{\text{end}}}\left(t_{\mathcal{M},m}^{t\text{end}}\right) = \Theta_2\left(t_{\mathcal{M},m}^{t\text{end}}\right), \quad l = 0, \dots, \mathcal{M},\\
&\sum_{\substack{l,r_1=0,\dots,\mathcal{N}\\ r_2=0,\dots,\mathcal{M}}} \varsigma_{r_1,r_2}\mathcal{G}_{r_1}(1)\mathcal{G}_{r_2}^{t_{\text{end}}}\left(t_{\mathcal{M},m}^{t\text{end}}\right) = \Theta_3\left(t_{\mathcal{M},m}^{t\text{end}}\right), \quad l = 0, \dots, \mathcal{M}.
\end{aligned} \tag{2.12}$$

An algebraic equations system is produced by combining Eqs. (2.11) and (2.12), and it is easy to solve.

2.2 Distributed and Riesz fractional Schrödinger equation

To address the TDSRFSP, GLLCT and GRLCT are developed

$$\begin{aligned}
&i\int_0^1 \kappa(\mu)\,{}_0^c\mathcal{D}_t^{\mu}\psi(x,t)\,d\mu + \varepsilon(-\Delta)^{\frac{\delta}{2}}\psi(x,t) + \left|\psi(x,t)\right|^2\psi(x,t)\\
&\quad = \Lambda(x,t), \quad (x,t) \in \Lambda^{\bullet} \times \Lambda^{\diamond},
\end{aligned} \tag{2.13}$$

where $\Lambda^{\bullet} \equiv [-1, 1]$ and $\Lambda^{\diamond} \equiv [0, t_{\text{end}}]$. Related to

$$\begin{aligned}
&\psi(x,0) = \Theta_1(x), \quad x \in \Lambda^{\bullet},\\
&\psi(0,t) = \Theta_2(t), \qquad \psi(x_{\text{end}},t) = \Theta_3(t), \quad t \in \Lambda^{\diamond}.
\end{aligned} \tag{2.14}$$

Firstly, we split $\psi(x,t)$ into its real and imaginary functions $\mathcal{U}(x,t)$ and $\mathcal{V}(x,t)$ as $\psi(x,t) = \mathcal{U}(x,t) + i\mathcal{U}(x,t)$. Based on this transformation, we get

$$\begin{aligned}
&\int_0^1 \kappa(\mu)\,{}_0^c\mathcal{D}_t^{\mu}\mathcal{U}(x,t)\,d\mu + \varepsilon(-\Delta)^{\frac{\delta}{2}}\mathcal{V}(x,t) + \left(\mathcal{U}^2(x,t) + \mathcal{V}^2(x,t)\right)\mathcal{V}(x,t)\\
&\quad = \Lambda_2(x,t), \quad (x,t) \in \Lambda^{\bullet} \times \Lambda^{\diamond},\\
&-\int_0^1 \kappa(\mu)\,{}_0^c\mathcal{D}_t^{\mu}\mathcal{V}(x,t)\,d\mu + \varepsilon(-\Delta)^{\frac{\delta}{2}}\mathcal{U}(x,t) + \left(\mathcal{U}^2(x,t) + \mathcal{V}^2(x,t)\right)\mathcal{U}(x,t)\\
&\quad = \Lambda_1(x,t), \quad (x,t) \in \Lambda^{\bullet} \times \Lambda^{\diamond},
\end{aligned} \tag{2.15}$$

where $\Lambda(x,t) = \Lambda_2(x,t) + i\Lambda_2(x,t)$, $\Lambda^{\bullet} \equiv [-1, 1]$, and $\Lambda^{\diamond} \equiv [0, t_{\text{end}}]$. Related to

$$\begin{aligned}
&\mathcal{U}(x,0) = \theta_1(x), \qquad \mathcal{U}(0,t) = \theta_2(t), \qquad \mathcal{U}(x_{\text{end}},t) = \theta_3(t), \quad x \in \Lambda^{\bullet}, t \in \Lambda^{\diamond},\\
&\mathcal{U}(x,0) = \vartheta_1(x), \qquad \mathcal{U}(0,t) = \vartheta_2(t), \qquad \mathcal{U}(x_{\text{end}},t) = \vartheta_3(t), \quad x \in \Lambda^{\bullet}, t \in \Lambda^{\diamond},
\end{aligned} \tag{2.16}$$

where $\Theta \equiv \theta + i\vartheta$.

To convert the TDSRFP into a nonlinear algebraic system, the GLLCT and GRSLCT are used. The truncated solution is written as follows:

$$\begin{aligned}
&\mathcal{U}_{\mathcal{N},\mathcal{M}}(x,t) = \sum_{\substack{r_1=0,\dots,\mathcal{N}\\ r_2=0,\dots,\mathcal{M}}} \varsigma_{r_1,r_2}\mathcal{G}_{r_1}(x)\mathcal{G}_{r_2}^{t_{\mathrm{end}}}(t),\\
&\mathcal{V}_{\mathcal{N},\mathcal{M}}(x,t) = \sum_{\substack{r_1=0,\dots,\mathcal{N}\\ r_2=0,\dots,\mathcal{M}}} \sigma_{r_1,r_2}\mathcal{G}_{r_1}(x)\mathcal{G}_{r_2}^{t_{\mathrm{end}}}(t).
\end{aligned} \tag{2.17}$$

Therefore, according to the previous analysis, we get

$$\begin{aligned}
&\Upsilon_1\big(x_{\mathcal{N},n}, t_{\mathcal{M},m}^{t_{\mathrm{end}}}\big) = \Lambda_2\big(x_{\mathcal{N},n}, t_{\mathcal{M},m}^{t_{\mathrm{end}}}\big), \quad n = 1,\dots,\mathcal{N}-1, m = 1,\dots,\mathcal{M},\\
&\Upsilon_2\big(x_{\mathcal{N},n}, t_{\mathcal{M},m}^{t_{\mathrm{end}}}\big) = \Lambda_1\big(x_{\mathcal{N},n}, t_{\mathcal{M},m}^{t_{\mathrm{end}}}\big), \quad n = 1,\dots,\mathcal{N}-1, m = 1,\dots,\mathcal{M},
\end{aligned} \tag{2.18}$$

where

$$\begin{aligned}
\Upsilon_1(x,t) = {}& \sum_{\substack{r_1=0,\dots,\mathcal{N}\\ r_2=0,\dots,\mathcal{M}\\ r_3=0,\dots,\mathcal{Q}}} \varsigma_{r_1,r_2}\mathcal{G}_{r_1}(x)\mathcal{F}_{r_2,r_3}^{t_{\mathrm{end}}}(t) + \varepsilon(-\Delta)^{\frac{\delta}{2}} \sum_{\substack{r_1=0,\dots,\mathcal{N}\\ r_2=0,\dots,\mathcal{M}}} \sigma_{r_1,r_2}\mathcal{G}_{r_1}(x)\mathcal{G}_{r_2}^{t_{\mathrm{end}}}(t)\\
&+ \Bigg(\sum_{\substack{r_1=0,\dots,\mathcal{N}\\ r_2=0,\dots,\mathcal{M}}} \varsigma_{r_1,r_2}\mathcal{G}_{r_1}(x)\mathcal{G}_{r_2}^{t_{\mathrm{end}}}(t)\Bigg)^2 \Bigg(\sum_{\substack{r_1=0,\dots,\mathcal{N}\\ r_2=0,\dots,\mathcal{M}}} \sigma_{r_1,r_2}\mathcal{G}_{r_1}(x)\mathcal{G}_{r_2}^{t_{\mathrm{end}}}(t)\Bigg)\\
&+ \Bigg(\sum_{\substack{r_1=0,\dots,\mathcal{N}\\ r_2=0,\dots,\mathcal{M}}} \sigma_{r_1,r_2}\mathcal{G}_{r_1}(x)\mathcal{G}_{r_2}^{t_{\mathrm{end}}}(t)\Bigg)^2 \Bigg(\sum_{\substack{r_1=0,\dots,\mathcal{N}\\ r_2=0,\dots,\mathcal{M}}} \sigma_{r_1,r_2}\mathcal{G}_{r_1}(x)\mathcal{G}_{r_2}^{t_{\mathrm{end}}}(t)\Bigg),\\
\Upsilon_2(x,t) = {}& -\sum_{\substack{r_1=0,\dots,\mathcal{N}\\ r_2=0,\dots,\mathcal{M}\\ r_3=0,\dots,\mathcal{Q}}} \sigma_{r_1,r_2}\mathcal{G}_{r_1}(x)\mathcal{F}_{r_2,r_3}^{t_{\mathrm{end}}}(t) + \varepsilon(-\Delta)^{\frac{\delta}{2}} \sum_{\substack{r_1=0,\dots,\mathcal{N}\\ r_2=0,\dots,\mathcal{M}}} \varsigma_{r_1,r_2}\mathcal{G}_{r_1}(x)\mathcal{G}_{r_2}^{t_{\mathrm{end}}}(t)\\
&+ \Bigg(\sum_{\substack{r_1=0,\dots,\mathcal{N}\\ r_2=0,\dots,\mathcal{M}}} \varsigma_{r_1,r_2}\mathcal{G}_{r_1}(x)\mathcal{G}_{r_2}^{t_{\mathrm{end}}}(t)\Bigg)^2 \Bigg(\sum_{\substack{r_1=0,\dots,\mathcal{N}\\ r_2=0,\dots,\mathcal{M}}} \varsigma_{r_1,r_2}\mathcal{G}_{r_1}(x)\mathcal{G}_{r_2}^{t_{\mathrm{end}}}(t)\Bigg)\\
&+ \Bigg(\sum_{\substack{r_1=0,\dots,\mathcal{N}\\ r_2=0,\dots,\mathcal{M}}} \sigma_{r_1,r_2}\mathcal{G}_{r_1}(x)\mathcal{G}_{r_2}^{t_{\mathrm{end}}}(t)\Bigg)^2 \Bigg(\sum_{\substack{r_1=0,\dots,\mathcal{N}\\ r_2=0,\dots,\mathcal{M}}} \varsigma_{r_1,r_2}\mathcal{G}_{r_1}(x)\mathcal{G}_{r_2}^{t_{\mathrm{end}}}(t)\Bigg).
\end{aligned}$$

In addition to

$$\begin{aligned}
&\sum_{\substack{l,r_1=0,\dots,\mathcal{N}\\ r_2=0,\dots,\mathcal{M}}} \varsigma_{r_1,r_2}\mathcal{G}_{r_1}(x_{\mathcal{N},n})\mathcal{G}_{r_2}^{t_{\mathrm{end}}}(0) = \theta_1(x_{\mathcal{N},n}), \quad k = 1,\dots,\mathcal{N}-1,\\
&\sum_{\substack{l,r_1=0,\dots,\mathcal{N}\\ r_2=0,\dots,\mathcal{M}}} \varsigma_{r_1,r_2}\mathcal{G}_{r_1}(-1)\mathcal{G}_{r_2}^{t_{\mathrm{end}}}\big(t_{\mathcal{M},m}^{t_{\mathrm{end}}}\big) = \theta_2\big(t_{\mathcal{M},m}^{t_{\mathrm{end}}}\big), \quad l = 0,\dots,\mathcal{M},\\
&\sum_{\substack{l,r_1=0,\dots,\mathcal{N}\\ r_2=0,\dots,\mathcal{M}}} \varsigma_{r_1,r_2}\mathcal{G}_{r_1}(1)\mathcal{G}_{r_2}^{t_{\mathrm{end}}}\big(t_{\mathcal{M},m}^{t_{\mathrm{end}}}\big) = \theta_3\big(t_{\mathcal{M},m}^{t_{\mathrm{end}}}\big), \quad l = 0,\dots,\mathcal{M},
\end{aligned} \tag{2.19}$$

$$\sum_{\substack{l,r_1=0,\dots,\mathcal{N}\\ r_2=0,\dots,\mathcal{M}}} \sigma_{r_1,r_2}\mathcal{G}_{r_1}(x_{\mathcal{N},n})\mathcal{G}_{r_2}^{t_{\text{end}}}(0) = \vartheta_1(x_{\mathcal{N},n}), \quad k = 1,\dots,\mathcal{N}-1,$$

$$\sum_{\substack{l,r_1=0,\dots,\mathcal{N}\\ r_2=0,\dots,\mathcal{M}}} \sigma_{r_1,r_2}\mathcal{G}_{r_1}(-1)\mathcal{G}_{r_2}^{t_{\text{end}}}\left(t_{\mathcal{M},m}^{t_{\text{end}}}\right) = \vartheta_2\left(t_{\mathcal{M},m}^{t_{\text{end}}}\right), \quad l = 0,\dots,\mathcal{M},$$

$$\sum_{\substack{l,r_1=0,\dots,\mathcal{N}\\ r_2=0,\dots,\mathcal{M}}} \sigma_{r_1,r_2}\mathcal{G}_{r_1}(1)\mathcal{G}_{r_2}^{t_{\text{end}}}\left(t_{\mathcal{M},m}^{t_{\text{end}}}\right) = \vartheta_3\left(t_{\mathcal{M},m}^{t_{\text{end}}}\right), \quad l = 0,\dots,\mathcal{M},$$

when Eqs. (2.18) and (2.19) are combined, we have a linear system of algebraic equations that is simple to solve.

3 Numerical results

We demonstrate the spectral collocation scheme's resilience and accuracy by applying the technique to three test problems.

Example 1 The convection–diffusion equation [57] is first presented

$$\begin{aligned}&\int_0^1 \Gamma(3-\mu)\,{}_0^c\mathcal{D}_t^{\mu}\mathcal{U}(x,t)\,d\mu + \frac{\Gamma(8-\delta)}{\Gamma(8)}(-\Delta)^{\frac{\delta}{2}}\mathcal{U}(x,t)\\ &\quad = \Delta(x,t), \quad (x,t)\in[-1,1]\times[0,0.5],\end{aligned} \tag{3.1}$$

the conditions and $\Delta(x,t)$ are given where $\mathcal{U}(x,t) = t^2(x^2-1)^4$.

Table 1 compares our results to those in [57] for various parameter values based on L_2-errors. Based on these findings, the recommended technique delivers superior numerical results than those reported in [57]. It is also worth mentioning that excellent predictions are made. The numerical solution and absolute errors of problem (1) are shown in Figs. 1 and 2, respectively. We showed the x-direction curves of numerical and precise solutions in Fig. 3, where $\delta = 1.8$, $\mathcal{N} = 8$, and $\mathcal{M} = 2$. Figures 4 and 5 depict the x- and t-graphs associated with absolute errors, respectively.

Table 1 L_2-comparison for problem (1)

Our spectral results at $\mathcal{M} = 2$ and different values of $\mathcal{N}$			
δ	4	6	8
1.2	3.38359×10^{-3}	7.23926×10^{-4}	1.7081×10^{-12}
1.4	3.78916×10^{-3}	9.39218×10^{-4}	5.07319×10^{-13}
1.8	4.77345×10^{-3}	1.74284×10^{-3}	1.17669×10^{-12}

Local discontinuous Galerkin method [57]					
	K	5	10	15	20
$N = 1$	1.2	$5.97 \times e^{-02}$	$8.6 \times e^{-03}$	$3.4 \times e^{-03}$	$1.8 \times e^{-03}$
	1.4	$2.84 \times e^{-02}$	$5.8 \times e^{-03}$	$2.5 \times e^{-03}$	$1.3 \times e^{-03}$
	1.8	$1.91 \times e^{-02}$	$4.5 \times e^{-03}$	$1.9 \times e^{-03}$	$9.9 \times e^{-04}$
$N = 2$	1.2	$3.52 \times e^{-02}$	$4.3 \times e^{-03}$	$1.2 \times e^{-03}$	$4.8 \times e^{-04}$
	1.4	$1.57 \times e^{-02}$	$2.1 \times e^{-03}$	$5.9 \times e^{-04}$	$2.6 \times e^{-04}$
	1.8	$1.45 \times e^{-02}$	$1.8 \times e^{-03}$	$5.5 \times e^{-04}$	$2.2 \times e^{-04}$

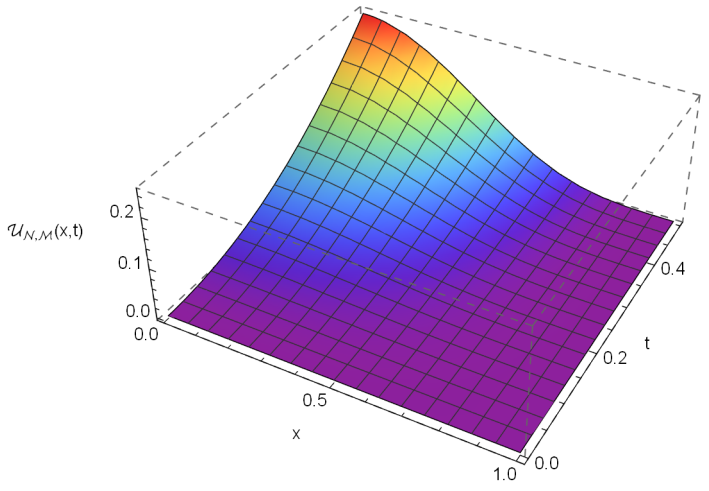

Figure 1 $\mathcal{U}_{\mathcal{N},\mathcal{M}}$ of Eq. (1) with $\delta = 1.8, \mathcal{N} = 8, \mathcal{M} = 2$

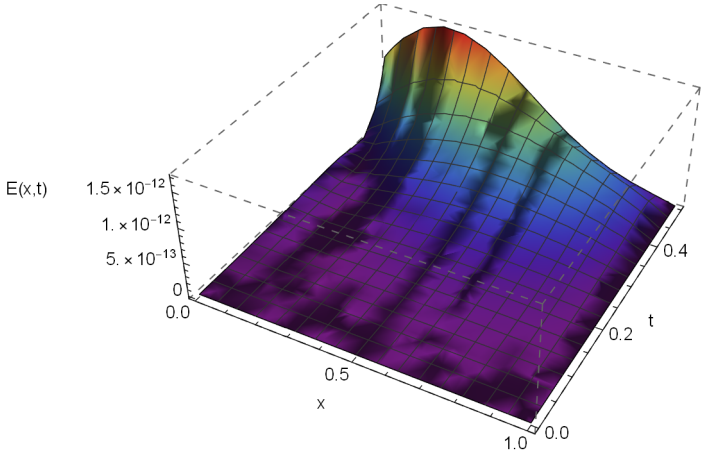

Figure 2 $E(x,t)$ of Eq. (1) with $\delta = 1.8, \mathcal{N} = 8, \mathcal{M} = 2$

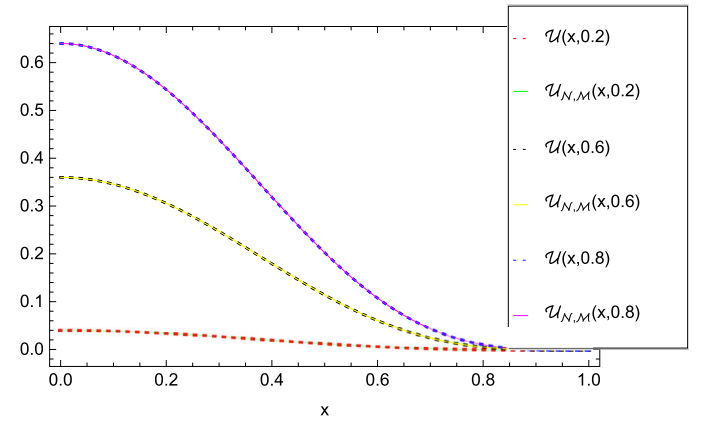

Figure 3 x-direction curves of $\mathcal{U}$ and $\mathcal{U}_{\mathcal{N},\mathcal{M}}$ of problem (1) with $\delta = 1.8, \mathcal{N} = 8, \mathcal{M} = 2$

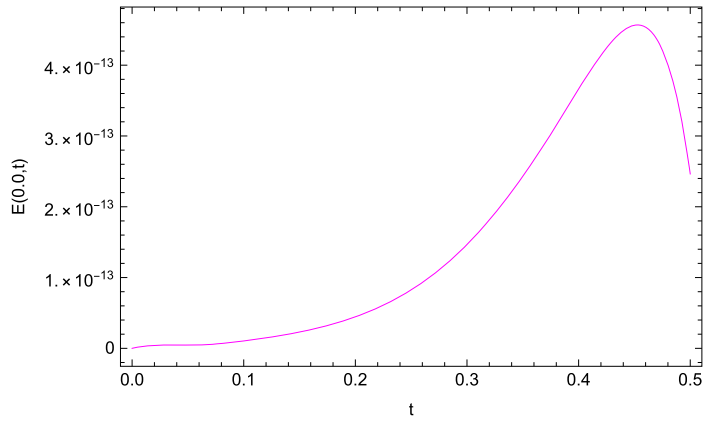

Figure 4 $E(0,t)$ of problem (1) with $\delta = 1.8, \mathcal{N} = 8, \mathcal{M} = 2$

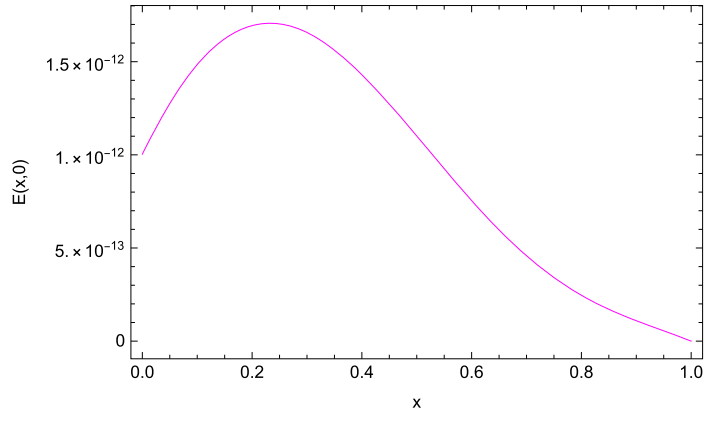

Figure 5 $E(x,0)$ of problem (1) with $\delta = 1.8, \mathcal{N} = 8, \mathcal{M} = 2$

Example 2 We introduce the temporal distributed and spatial Riesz Burgers' equation [57]

$$\begin{aligned}&\int_0^1 \Gamma(3-\mu)\,{}_0^c\mathcal{D}_t^{\mu}\mathcal{U}(x,t)\,d\mu + \frac{\Gamma(8-\delta)}{\Gamma(8)}(-\Delta)^{\frac{\delta}{2}}\mathcal{U}(x,t) + \frac{\partial}{\partial x}\left(\frac{(\mathcal{U}(x,t))^2}{2}\right)\\ &\quad = \Delta(x,t), \quad (x,t) \in [-1,1]\times[0,0.5],\end{aligned} \tag{3.2}$$

$\Delta(x,t)$ and conditions are provided, $\mathcal{U}(x,t) = t^2(x^2-1)^4$.

Table 2 shows a comparison of our results with those in [57] at different parameter values based on L_2-errors. The suggested approach produces superior numerical results to those published in [57] based on these findings. It is also worth noting that great estimates are made.

Table 2 L_2-comparison for problem (2)

Our spectral results at $\mathcal{M}=2$ and different values of $\mathcal{N}$					
δ	4		6		8
1.2	3.70018×10^{-3}		1.01319×10^{-3}		1.69633×10^{-12}
1.4	4.09205×10^{-3}		1.19241×10^{-3}		5.02948×10^{-13}
1.8	5.05627×10^{-3}		1.9247×10^{-3}		1.15406×10^{-12}
Local discontinuous Galerkin method [57]					
	K	5	10	15	20
$N=1$	1.2	$7.8 \times e^{-3}$	$1.9 \times e^{-3}$	$2.048.5 \times e^{-4}$	$4.6 \times e^{-4}$
	1.4	$4.9 \times e^{-3}$	$1.1 \times e^{-3}$	$4.6 \times e^{-4}$	$2.152.5 \times e^{-4}$
	1.8	$1.9 \times e^{-3}$	$5.1 \times e^{-4}$	$2.2 \times e^{-4}$	$1.2 \times e^{-4}$
$N=2$	1.2	$3.4 \times e^{-3}$	$4.2 \times e^{-4}$	$1.3 \times e^{-4}$	$5.2 \times e^{-5}$
	1.4	$1.3 \times e^{-3}$	$1.8 \times e^{-4}$	$5.6 \times e^{-5}$	$2.5 \times e^{-5}$
	1.8	$8.2 \times e^{-4}$	$1.1 \times e^{-4}$	$3.1 \times e^{-5}$	$1.3 \times e^{-8}$

Table 3 L_2-comparison for problem (3)

Our spectral results at $\mathcal{M}=2$ and different values of $\mathcal{N}$					
δ	4	6	8	10	
1.2	3.37831×10^{-3}	1.01074×10^{-3}	1.22583×10^{-4}	3.61583×10^{-12}	
1.4	3.50039×10^{-3}	1.12899×10^{-3}	1.42245×10^{-4}	3.35625×10^{-12}	
1.8	3.70169×10^{-3}	1.39914×10^{-3}	1.88913×10^{-4}	1.76056×10^{-12}	
Local discontinuous Galerkin method [57]					
	K	5	10	15	20
$N=1$	1.2	$1.23e^{-02}$	$4.61e^{-03}$	$1.97e^{-03}$	$1.1e^{-03}$
	1.4	$1.01e^{-02}$	$2.51e^{-03}$	$1.11e^{-03}$	$6.31e^{-04}$
	1.8	$7.31e^{-03}$	$1.91e^{-03}$	$8.35e^{-04}$	$4.71e^{-04}$
$N=2$	1.2	$8.35e^{-03}$	$1.21e^{-03}$	$3.55e^{-04}$	$1.41e^{-04}$
	1.4	$6.24e^{-03}$	$9.23e^{-04}$	$2.79e^{-04}$	$1.13e^{-04}$
	1.8	$2.62e^{-03}$	$3.54e^{-04}$	$1.13e^{-04}$	$4.66e^{-05}$

Example 3 We introduce the temporal distributed and spatial Riesz convection–diffusion and Schrödinger-type equation [57]

$$\begin{aligned}&\int_0^1 \Gamma(3-\mu)\,{}_0^c\mathcal{D}_t^{\mu}\psi(x,t)\,d\mu - \frac{\Gamma(10-\delta)}{\Gamma(10)}(-\Delta)^{\frac{\delta}{2}}\psi(x,t) + \big|\psi(x,t)\big|^2\psi(x,t)\\ &\quad = \Delta(x,t), \quad (x,t)\in[-1,1]\times[0,0.5],\end{aligned} \tag{3.3}$$

$\Delta(x,t)$ and conditions are provided $\psi(x,t) = t^2(1+i)(x^2-1)^5$.

Table 3 shows a comparison of our results with those in [57] at different parameter values based on L_2-errors. The suggested approach produces superior numerical results to those published in [57] based on these findings. It is also worth noting that great estimates are made.

We see in Figs. 6 and 7 the absolute errors of problem (3) for both real and imaginary parts, respectively. In Figs. 8 and 9, we plotted the x-direction curves of numerical and exact solutions for both real and imaginary parts, respectively, where $\delta = 1.8$, $\mathcal{N} = 10$, $\mathcal{M} = 2$; while the x-graphs related to the absolute errors are sketched in Figs. 10 and 11 for both real and imaginary parts, respectively.

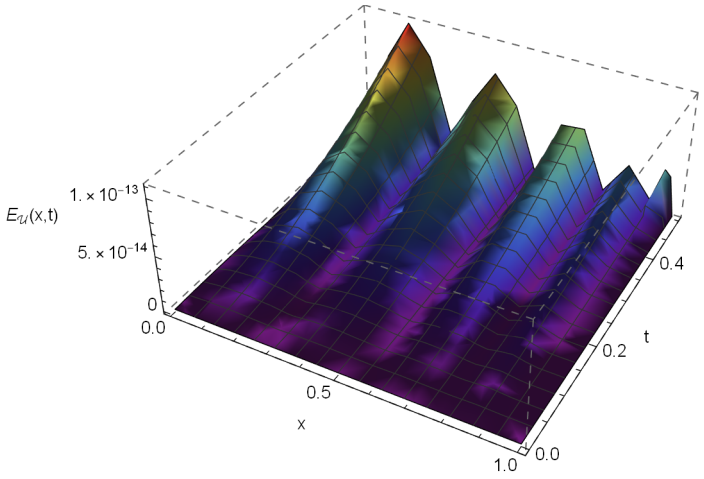

Figure 6 $E_{\mathcal{U}}$ of problem (3), with $\delta = 1.8$, $\mathcal{N} = 10$, $\mathcal{M} = 2$

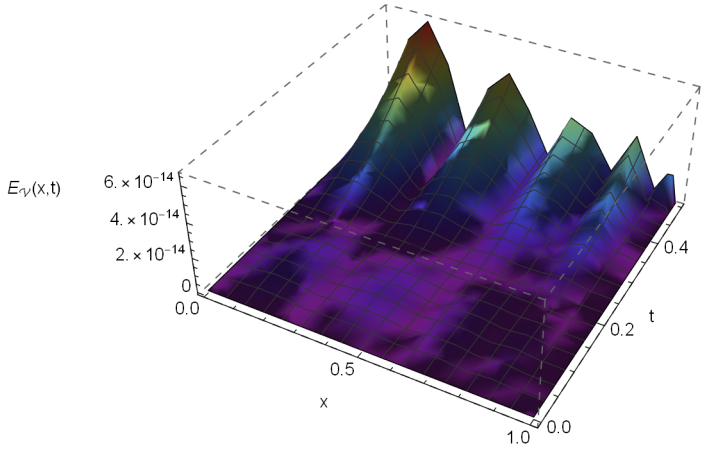

Figure 7 $E_{\mathcal{V}}(x,t)$ of problem (3) with $\delta = 1.8$, $\mathcal{N} = 10$, $\mathcal{M} = 2$

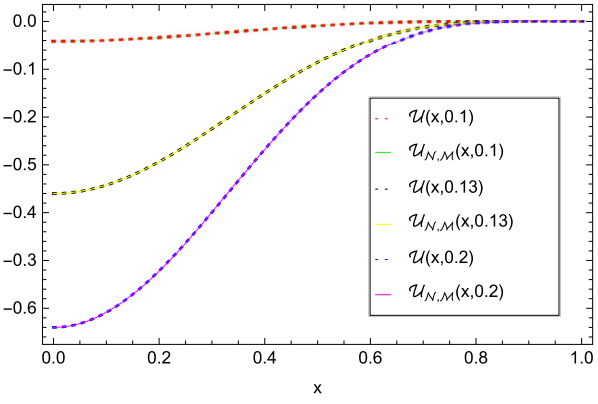

Figure 8 x-direction curves of $\mathcal{U}$ and $\mathcal{U}_{\mathcal{N},\mathcal{M}}$ of problem (3), where $\delta = 1.8$, $\mathcal{N} = 10$, $\mathcal{M} = 2$

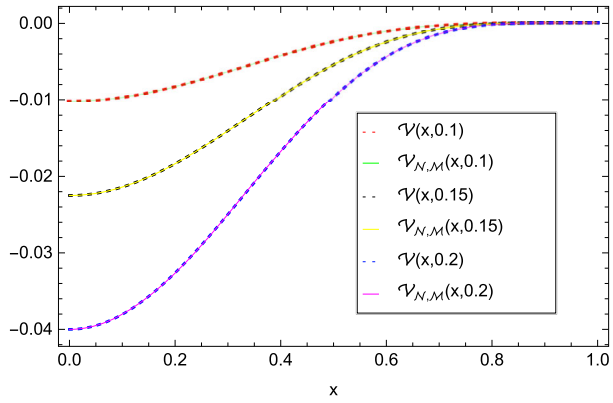

Figure 9 *x*-direction curves of $\mathcal{V}$ and $\mathcal{V}_{\mathcal{N},\mathcal{M}}$ of problem (3), where $\delta = 1.8, \mathcal{N} = 10, \mathcal{M} = 2$

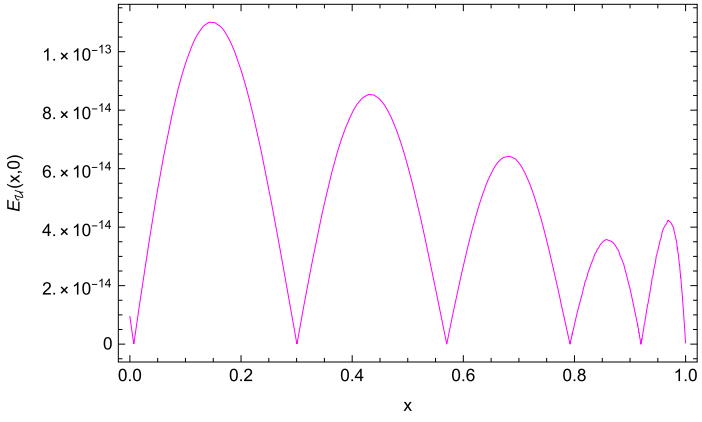

Figure 10 $E_{\mathcal{U}}(x,0)$ of problem of problem (3), where $\delta = 1.8, \mathcal{N} = 10, \mathcal{M} = 2$

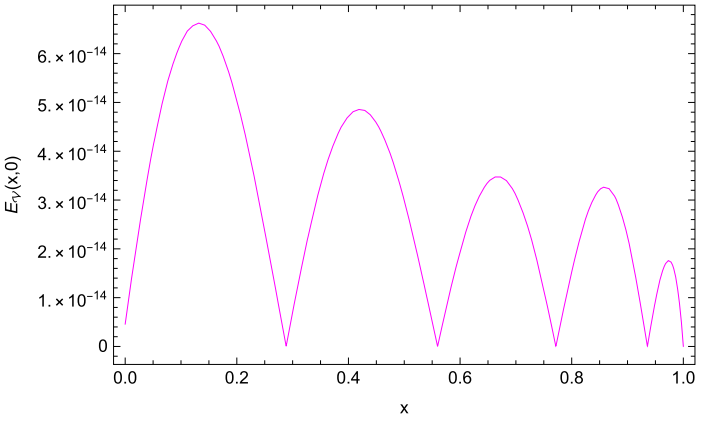

Figure 11 $E_{\mathcal{V}}(x,0)$ of problem (3), where $\delta = 1.8, \mathcal{N} = 10, \mathcal{M} = 2$

4 Conclusion

We present an extraordinarily accurate collocation approach for convection–diffusion and Schrodinger-type equations for mixed Riesz and distributed fractional order. A comprehensive theoretical description as well as a series of numerical tests to demonstrate the technique's execution and eligibility are provided. We can see that our approach is highly accurate and reliable based on the findings. More fractional order issues can be included in the current theoretical debate. The current figures are completely consistent with the predicted outcomes of the spectral collocation technique, and there is clear evidence of exponential convergence. In this study, the GLLCT and GRSLCT approaches are employed to solve the given models. The shifted Legendre nodes are used as interpolation points for the independent variables, and the solution is represented as a series of shifted Legendre polynomials. After that, the residuals at the shifted Legendre quadrature points are estimated. As a consequence, we have an algebraic system that can be solved using a suitable method. A variety of numerical problems are used to illustrate the precision of the proposed technique. Due to their adaptability to both linear and nonlinear equations, the spectral collocation approach has become widely used to estimate many types of differential and integral equations. Since their global character fits well with the nonlocal notion of fractional operators, spectral techniques are excellent candidates for solving fractional differential equations. Spectral techniques provide a high degree of precision and exponential convergence rates. In the tables above, the cheap costs and excellent accuracy are readily visible. The suggested approach is efficient and accurate according to simulation results.

Acknowledgements
The authors extend their appreciation to the Deanship of Scientific Research at Imam Mohammad Ibn Saud Islamic University for funding this work through Research Group no. RG-21-09-07.

Funding
The authors extend their appreciation to the Deanship of Scientific Research at Imam Mohammad Ibn Saud Islamic University for funding this work through Research Group no. RG-21-09-07.

Availability of data and materials
Not applicable.

Declarations

Competing interests
The authors declare that they have no competing interests.

Authors' contributions
The authors declare that the study was realized in collaboration with equal responsibility. All authors read and approved the final manuscript.

Publisher's Note

Springer Nature remains neutral with regard to jurisdictional claims in published maps and institutional affiliations.

Received: 19 October 2021 Accepted: 8 February 2022 Published online: 18 March 2022

References

1. Singh, S., Devi, V., Tohidi, E., Singh, V.K.: An efficient matrix approach for two-dimensional diffusion and telegraph equations with Dirichlet boundary conditions. Phys. A, Stat. Mech. Appl. **545**, 123784 (2020)
2. Yang, Y., Rządkowski, G., Pasban, A., Tohidi, E., Shateyi, S.: A high accurate scheme for numerical simulation of two-dimensional mass transfer processes in food engineering. Alex. Eng. J. **60**(2), 2629–2639 (2021)
3. Papageorgiou, N.S., Rădulescu, V.D., Repovš, D.D.: Nonlinear Analysis—Theory and Methods. Springer, Berlin (2019)
4. Herrmann, R.: Fractional Calculus: An Introduction for Physicists. World Scientific, Singapore (2014)

5. Tarasov, V.E.: Fractional Dynamics: Applications of Fractional Calculus to Dynamics of Particles, Fields and Media. Springer, Berlin (2011)
6. West, B.J.: Fractional Calculus View of Complexity: Tomorrow's Science. CRC Press, Boca Raton (2016)
7. Kilbas, A.: Theory and applications of fractional differential equations
8. West, B.J.: Nature's Patterns and the Fractional Calculus, vol. 2. de Gruyter, Berlin (2017)
9. Liu, Y.: A new method for converting boundary value problems for impulsive fractional differential equations to integral equations and its applications. Adv. Nonlinear Anal. **8**(1), 386–454 (2019)
10. Seki, K., Wojcik, M., Tachiya, M.: Fractional reaction–diffusion equation. J. Chem. Phys. **119**(4), 2165–2170 (2003)
11. Baleanu, D., Magin, R.L., Bhalekar, S., Daftardar-Gejji, V.: Chaos in the fractional order nonlinear Bloch equation with delay. Commun. Nonlinear Sci. Numer. Simul. **25**(1–3), 41–49 (2015)
12. Podlubny, I.: Fractional Differential Equations: An Introduction to Fractional Derivatives, Fractional Differential Equations, to Methods of Their Solution and Some of Their Applications. Elsevier, Amsterdam (1998)
13. Hadadian, M., Yousefi, N., Ghoreishi Najafabadi, S.H., Tohidi, E.: A fast and efficient numerical approach for solving advection–diffusion equations by using hybrid functions. Comput. Appl. Math. **38**(4), 1–19 (2019)
14. Hadadian, M., Yousefi, N., Ghoreishi Najafabadi, S.H., Tohidi, E.: A new spectral integral equation method for solving two-dimensional unsteady advection–diffusion equations via Chebyshev polynomials. Eng. Comput. **36**(7), 2327–2368 (2019)
15. Chechkin, A.V., Gorenflo, R., Sokolov, I.M.: Retarding subdiffusion and accelerating superdiffusion governed by distributed-order fractional diffusion equations. Phys. Rev. E **66**(4), 046129 (2002)
16. Mashayekhi, S., Razzaghi, M.: Numerical solution of distributed order fractional differential equations by hybrid functions. J. Comput. Phys. **315**, 169–181 (2016)
17. Bayın, S.Ş.: Consistency problem of the solutions of the space fractional Schrödinger equation. J. Math. Phys. **54**(9), 092101 (2013)
18. Chen, H., Lü, S., Chen, W.: Finite difference/spectral approximations for the distributed order time fractional reaction–diffusion equation on an unbounded domain. J. Comput. Phys. **315**, 84–97 (2016)
19. Li, X.Y., Wu, B.Y.: A numerical method for solving distributed order diffusion equations. Appl. Math. Lett. **53**, 92–99 (2016)
20. Hafez, R.M., Zaky, M.A., Abdelkawy, M.A.: Jacobi spectral Galerkin method for distributed-order fractional Rayleigh–Stokes problem for a generalized second grade fluid. Front. Phys. **7**, 240 (2020)
21. Abdelkawy, M.A., et al.: Numerical solutions for fractional initial value problems of distributed-order. Int. J. Mod. Phys. C **32**(07), 1–13 (2021)
22. Abdelkawy, M.A., Babatin, M.M., Lopes, A.M.: Highly accurate technique for solving distributed-order time-fractional-sub-diffusion equations of fourth order. Comput. Appl. Math. **39**(2), 1–22 (2020)
23. Abdelkawy, M.A.: An improved collocation technique for distributed-order fractional partial differential equations. Rom. Rep. Phys. **72**, 104 (2020)
24. Abdelkawy, M.A., Lopes, A.M., Zaky, M.A.: Shifted fractional Jacobi spectral algorithm for solving distributed order time-fractional reaction–diffusion equations. Comput. Appl. Math. **2**(38), 1–21 (2019)
25. Abdelkawy, M.A.: A collocation method based on Jacobi and fractional order Jacobi basis functions for multi-dimensional distributed-order diffusion equations. Int. J. Nonlinear Sci. Numer. Simul. **19**(7–8), 781–792 (2018)
26. Li, J., Liu, F., Feng, L., Turner, I.: A novel finite volume method for the Riesz space distributed-order diffusion equation. Comput. Math. Appl. **74**(4), 772–783 (2017)
27. Fan, W., Liu, F.: A numerical method for solving the two-dimensional distributed order space-fractional diffusion equation on an irregular convex domain. Appl. Math. Lett. **77**, 114–121 (2018)
28. Jia, J., Wang, H.: A fast finite difference method for distributed-order space-fractional partial differential equations on convex domains. Comput. Math. Appl. **75**(6), 2031–2043 (2018)
29. Chen, F., Baleanu, D., Wu, G.-C.: Existence results of fractional differential equations with Riesz–Caputo derivative. Eur. Phys. J. Spec. Top. **226**(16), 3411–3425 (2017)
30. Arshad, S., Baleanu, D., Huang, J., Al Qurashi, M.M., Tang, Y., Zhao, Y.: Finite difference method for time-space fractional advection–diffusion equations with Riesz derivative. Entropy **20**(5), 321 (2018)
31. Agrawal, O.P.: Fractional variational calculus in terms of Riesz fractional derivatives. J. Phys. A, Math. Theor. **40**(24), 6287 (2007)
32. Frederico, G.S.F., Torres, D.F.M.: Fractional Noether's theorem in the Riesz–Caputo sense. Appl. Math. Comput. **217**(3), 1023–1033 (2010)
33. Almeida, R.: Fractional variational problems with the Riesz–Caputo derivative. Appl. Math. Lett. **25**(2), 142–148 (2012)
34. Meerschaert, M.M., Tadjeran, C.: Finite difference approximations for fractional advection–dispersion flow equations. J. Comput. Appl. Math. **172**(1), 65–77 (2004)
35. Yang, Q., Liu, F., Turner, I.: Numerical methods for fractional partial differential equations with Riesz space fractional derivatives. Appl. Math. Model. **34**(1), 200–218 (2010)
36. Sousa, E.: A second order explicit finite difference method for the fractional advection diffusion equation. Comput. Math. Appl. **64**(10), 3141–3152 (2012)
37. Tian, W., Zhou, H., Deng, W.: A class of second order difference approximations for solving space fractional diffusion equations. Math. Comput. **84**(294), 1703–1727 (2015)
38. Ding, H., Li, C., Chen, Y.: High-order algorithms for Riesz derivative and their applications (ii). J. Comput. Phys. **293**, 218–237 (2015)
39. Wang, X., Liu, F., Chen, X.: Novel second-order accurate implicit numerical methods for the Riesz space distributed-order advection–dispersion equations. Adv. Math. Phys. **2015**, 590435 (2015)
40. Zheng, X., Liu, H., Wang, H., Fu, H.: An efficient finite volume method for nonlinear distributed-order space-fractional diffusion equations in three space dimensions. J. Sci. Comput. **80**(3), 1395–1418 (2019)
41. Bhrawy, A.H., Zaky, M.A.: Highly accurate numerical schemes for multi-dimensional space variable-order fractional Schrödinger equations. Comput. Math. Appl. **73**(6), 1100–1117 (2017)
42. Bhrawy, A.H., Zaky, M.A.: An improved collocation method for multi-dimensional space-time variable-order fractional Schrödinger equations. Appl. Numer. Math. **111**, 197–218 (2017)

43. Huang, Y., Noori Skandari, M.H., Mohammadizadeh, F., Tehrani, H.A., Georgiev Georgiev, S., Tohidi, E., Shateyi, S.: Space-time spectral collocation method for solving Burgers equations with the convergence analysis. Symmetry **11**(12), 1439 (2019)
44. Nejad Yousefi, M.H., Ghoreishi Najafabadi, S.H., Tohidi, E.: A new WENO based Chebyshev spectral volume method for solving one-and two-dimensional conservation laws. J. Comput. Phys. **403**, 109055 (2020)
45. Zogheib, B., Tohidi, E.: Modal Hermite spectral collocation method for solving multi-dimensional hyperbolic telegraph equations. Comput. Math. Appl. **75**(10), 3571–3588 (2018)
46. Zogheib, B., Tohidi, E.: An accurate space-time pseudospectral method for solving nonlinear multi-dimensional heat transfer problems. Mediterr. J. Math. **14**(1), 30 (2017)
47. Bhrawy, A.H.: An efficient Jacobi pseudospectral approximation for nonlinear complex generalized Zakharov system. Appl. Math. Comput. **247**, 30–46 (2014)
48. Bhrawy, A.H.: A Jacobi spectral collocation method for solving multi-dimensional nonlinear fractional sub-diffusion equations. Numer. Algorithms **73**(1), 91–113 (2016)
49. Abdelkawy, M.A., Amin, A.Z.M., Bhrawy, A.H., Tenreiro Machado, J.A., Lopes, A.M.: Jacobi collocation approximation for solving multi-dimensional Volterra integral equations. Int. J. Nonlinear Sci. Numer. Simul. **18**(5), 411–425 (2017)
50. Doha, E.H., Bhrawy, A.H., Abdelkawy, M.A., Van Gorder, R.A.: Jacobi–Gauss–Lobatto collocation method for the numerical solution of 1 + 1 nonlinear Schrödinger equations. J. Comput. Phys. **261**, 244–255 (2014)
51. Bhrawy, A.H., Zaky, M.A., Baleanu, D.: New numerical approximations for space-time fractional Burgers' equations via a Legendre spectral-collocation method. Rom. Rep. Phys. **67**(2), 340–349 (2015)
52. Huang, Y., Mohammadi Zadeh, F., Noori Skandari, M.H., Tehrani, H.A., Tohidi, E.: Space-time Chebyshev spectral collocation method for nonlinear time-fractional Burgers equations based on efficient basis functions. Math. Methods Appl. Sci. **44**(5), 4117–4136 (2021)
53. Yang, Y., Wang, J., Zhang, S., Tohidi, E.: Convergence analysis of space-time Jacobi spectral collocation method for solving time-fractional Schrödinger equations. Appl. Math. Comput. **387**, 124489 (2020)
54. Canuto, C., Hussaini, M.Y., Quarteroni, A., Zang, T.A.: Spectral Methods: Fundamentals in Single Domains. Springer, Berlin (2007)
55. Bhrawy, A.H., Abdelkawy, M.A., Tenreiro Machado, J., Amin, A.Z.M.: Legendre–Gauss–Lobatto collocation method for solving multi-dimensional Fredholm integral equations. Comput. Math. Appl. (2016)
56. Bhrawy, A.H., Zaky, M.A., Van Gorder, R.A.: A space-time Legendre spectral tau method for the two-sided space-time Caputo fractional diffusion-wave equation. Numer. Algorithms **71**(1), 151–180 (2016)
57. Aboelenen, T.: Local discontinuous Galerkin method for distributed-order time and space-fractional convection–diffusion and Schrödinger-type equations. Nonlinear Dyn. **92**(2), 395–413 (2018)
58. Bhrawy, A.H., Abdelkawy, M.A.: A fully spectral collocation approximation for multi-dimensional fractional Schrödinger equations. J. Comput. Phys. **294**, 462–483 (2015)
59. Abd-Elhameed, W.M., Youssri, Y.H.: Connection formulae between generalized Lucas polynomials and some Jacobi polynomials: application to certain types of fourth-order BVPs. Int. J. Appl. Comput. Math. **6**(2), 1–19 (2020)
60. Youssri, Y.H., Hafez, R.M.: Exponential Jacobi spectral method for hyperbolic partial differential equations. Math. Sci. **13**(4), 347–354 (2019)

Submit your manuscript to a SpringerOpen journal and benefit from:

- ► Convenient online submission
- ► Rigorous peer review
- ► Open access: articles freely available online
- ► High visibility within the field
- ► Retaining the copyright to your article

Submit your next manuscript at ► springeropen.com